DALTON
FULL PAPER

Characterization of novel redox-active triruthenium(III) complexes with a disulfide alkyl ligand. Anion-dependent redox behaviour of monolayer assemblies on gold †

Masaaki Abe,* Akira Sato, Tomohiko Inomata, Toshihiro Kondo, Kohei Uosaki * and Yoichi Sasaki *

Division of Chemistry, Graduate School of Science, Hokkaido University, Kita-ku, Sapporo 060-0810, Japan. E-mail: mabe@sci.hokudai.ac.jp

Received 15th March 2000, Accepted 27th June 2000
Published on the Web 27th July 2000

New oxo-centred acetate-bridged triruthenium(III) complexes with a long alkyl-chain disulfide ligand, (NC_5H_4)-$CH_2NHC(O)(CH_2)_nSS(CH_2)_nC(O)NHCH_2(C_5H_4N)$ (C_5H_4N represents a 4-pyridyl residue, $n = 10$; abbreviated as C10PY), have been prepared as a redox-active metal cluster adsorbate on gold electrodes: $[Ru_3(O)(CH_3CO_2)_6(mpy)_2$-$(C10PY)]ClO_4$ **5a** (mpy = 4-methylpyridine), $[Ru_3(O)(CH_3CO_2)_6(mpy)_2(C10PY)]CF_3SO_3$ **5b**. The preparation, spectroscopic and electrochemical properties of **5a**,**5b** are presented and are compared with those of triruthenium(III) analogues of a shorter alkyl-chain disulfide ligand ($n = 2$; abbreviated as C2PY), *e.g.* $[Ru_3(O)(CH_3CO_2)_6(mpy)_2(C2PY)]$-$ClO_4$ **3a** and $[Ru_3(O)(CH_3CO_2)_6(MeIm)_2(C2PY)]ClO_4$ **4a** (MeIm = 1-methylimidazole). Characterization of all the compounds was accomplished using ^1H and ^1H–^1H COSY NMR, UV-vis and infrared spectroscopy, elemental analysis, fast-atom bombardment (FAB) mass spectrometry and cyclic voltammetry. Compounds **3a**, **4a** and **5a**,**5b** in 0.1 M $[n\text{-}Bu_4N]PF_6$–CH_3CN exhibit three $\{Ru_3(O)\}$ cluster core-based one-electron redox waves which are all reversible in the applied potential range between +1.2 and –2.0 V *vs.* Ag–AgCl. The redox potentials are dependent on the basicity of the terminal ligands (mpy and MeIm), but are insensitive to the length of the methylene chains of the disulfide ligand (C10PY and C2PY). Self-assembly of **5b** on a gold electrode results in the formation of electrochemically stable monolayers which exhibit one-electron redox wave corresponding to the Ru_3 redox process III,III,III–II,III,III in aqueous media containing 0.1 M supporting electrolytes. The redox potentials and the shape of the voltammetric waves of the surface-attached triruthenium complexes are found to be largely dependent upon the nature of anions used (ClO_4^-, $CF_3SO_3^-$, NO_3^-, PF_6^- and SO_4^{2-}) and also upon the basicity of terminal ligands on the $\{Ru_3(O)\}$ cluster moiety.

Introduction

The construction of artificial supramolecular architectures on solid surfaces is currently of great interest and represents an important aspect of chemistry of self-assembly processes, since it offers highly ordered nanoscale structures with well defined chemical and physical properties.[1] Especially, the use of atomically flat electrode surfaces is a promising strategy to assemble redox-active molecular components.[2] The ability to vary terminal functionalities in self-assembled monolayers enables the modulation of the resulting interfacial properties. Transition-metal complexes with a thiol or a disulfide group are well studied adsorbates for modification of gold electrodes. So far, the development in the creation of two-dimensional arrays on gold surfaces has relied heavily on the use of mononuclear species, including ferrocene derivatives,[3,4] metalloporphyrins,[5] ruthenium(II),[6] osmium(II),[7] and rhenium(I)[8] complexes, while the self-assembly of multinuclear transition-metal complexes has been less common; only a few recent reports on the latter are available, *i.e.* monolayers of trinickel(II) clusters[9] and those of palladium(II)-based dendritic compounds.[10] Since, with an appropriate choice of metal ions and supporting ligands, multinuclear complexes can exhibit various interesting chemical properties (*i.e.* multiple redox processes, multicentre catalysis, *etc.*), further developments in the synthesis of new self-assembled monolayers of varied metal clusters is highly encouraged. In this regard, we have been preparing novel monolayer assemblies on gold electrodes using redox-active ruthenium and iron multinuclear complexes; examples include (μ-oxo)(μ-acetato)diiron(III) complexes,[11] (μ-oxo)bis-(μ-acetato)diruthenium(III) complexes,[12] (μ_3-oxo)hexakis-(μ-acetato)triruthenium(III) complexes[13] and mixed-valent triruthenium(II,III,III) complexes.[14] Among the series, proton-coupled electron-transfer reactions were observed for monolayers of the (μ-oxo)dimetal complexes,[11,12] as found for the discrete analogues dissolved in solution.[15]

The present study explores the preparation and electrochemistry of monolayers with (μ_3-oxo)hexakis(μ-acetato)triruthenium(III) cores, displaying a well defined reversible redox response in water media. The oxo-centred, acetate-bridged triruthenium complexes of the type $[Ru_3(O)(CH_3CO_2)_6L_3]^{n+}$ (L = a monodentate ligand)[16,17] constitute a well known class of transition-metal cluster compounds owing to their reversible multi-step redox chemistry.[18–20] Recent developments in these compounds include the preparation of Ru_3-based multi-component systems with multi-electron redox processes[21] and studies of intramolecular electron transfer,[22] photochemistry[23] and catalysis.[24] Thus, immobilization of the Ru_3 units may allow to form a novel surface systems with unique interfacial phenomena based upon the properties described above.

† Electronic supplementary information (ESI) available: FAB MS data for complexes **3a**, **4a** and **5b**. See http://www.rsc.org/suppdata/dt/b0/b002105i/

DOI: 10.1039/b002105i

This journal is © The Royal Society of Chemistry 2000

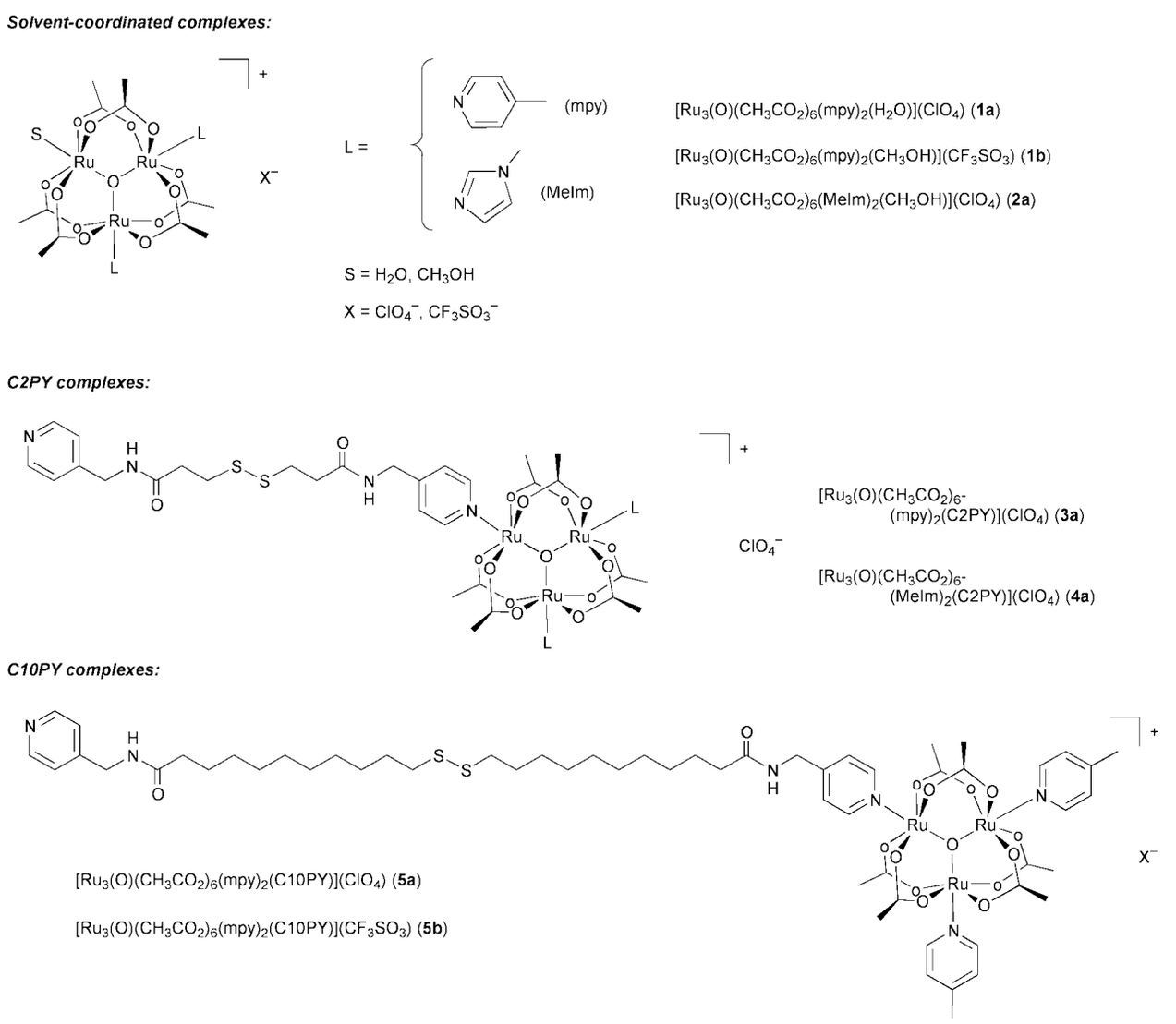

Fig. 1 Triruthenium(III) complexes in this study.

The complexes considered in this study are shown in Fig. 1. The ligand C2PY[8] and the new ligand C10PY possess two and ten methylene groups, respectively, between the disulfide group and pyridyl moieties. Solvent-co-ordinated complexes **1a**, **1b** and **2a** are the starting materials for C2PY complexes **3a**,**4a**[13] and the new C10PY complexes **5a**,**5b**.

In our previous paper[13] we reported cyclic voltammetric behaviour of self-assembled monolayers of C2PY complexes **3a** and **4a** on Au(111) electrodes. Complexes of a disulfide ligand with a longer alkyl chain (*e.g.* C10PY) are expected to form more stable and ordered monolayers due to enhanced van der Waals interactions between the neighboring alkyl chains compared to complexes with a shorter alkyl ligand (C2PY). Here we describe details of the spectroscopic and electrochemical characteristics of C10PY complexes **5a**,**5b** along with the corresponding properties of **1a**, **1b**, **2a**, **3a** and **4a**, previously not reported.[13] Further we examined the redox behaviour of a monolayer assembly of compound **5b** on a gold electrode under varied experimental conditions; emphasis is placed on the effects of supporting electrolytes and solution pH on the surface redox properties.

Results and discussion

Synthesis of triruthenium(III) complexes

Our preparative strategy to construct monolayers of triruthenium(III) complexes on gold electrodes is based on the preparation of triruthenium(III) complexes having a disulfide ligand as the anchoring group and subsequent attachment of those compounds through the formation of Au–S bonds.[2] In this study, new disulfide-functionalized triruthenium(III) complexes, $[Ru_3(O)(CH_3CO_2)_6(mpy)_2(C10PY)]ClO_4$ **5a** and $[Ru_3(O)(CH_3CO_2)_6(mpy)_2(C10PY)]CF_3SO_3$ **5b**, have been prepared and characterized (Fig. 1). The ligand C10PY contains a disulfide moiety with two pyridyl pendants at the termini which can co-ordinate to metal centres. The complexes containing C10PY are isolated as thermally stable, crystalline materials that are readily soluble in organic solvents including acetonitrile, methanol, and ethanol, but are insoluble in water.

NMR spectroscopy

^{1}H NMR spectroscopy provides firm evidence in complexes **5a** and **5b** for the 2 : 1 stoichiometry of mixed terminal ligands. The data are summarized in Table 1. Here, ^{1}H NMR data of C2PY complexes and solvent-co-ordinated complexes are also included for comparison.

The ^{1}H NMR spectrum of compound **5b** in CD_3CN at 20 °C is shown in Fig. 2(a) as a typical example, and the proton labeling scheme is given in Fig. 2(b). In spite of the paramagnetic nature of Ru^{III}_3 complexes, all the signals of **5b** are observed in the "diamagnetic" region in the ^{1}H NMR spectrum due to a significant antiferromagnetic coupling between d^5 ruthenium(III) centres through the central oxo group, as found in related complexes.[19] Two doublet signals at δ 8.46 (2 H) and

Table 1 ^{1}H NMR spectral data (270.15 MHz, CD_3CN, 20 °C)

Complex	Chemical shift (δ *vs.* TMS) and the signal assignments							
1b				mpy:	β″-H	4.89 (s, 4 H)	acetate CH_3:	6.33 (s, 6 H)
					α″-H	−1.58 (s, 4 H)		4.70 (s, 12 H)
					CH_3	2.88 (s, 6 H)		
2a				MeIm:		4.92 (s, 2 H)	acetate CH_3:	4.43 (s, 6 H)
						1.10 (s, br, 2 H)		2.14 (s, 12 H)
						0.17 (s, br, 2 H)		
					CH_3	4.77 (s, 6 H)	CH_3OH:	3.25 (s, 3 H)
3a	C2PY:	α-H	8.44 (d, 2 H)	mpy:	β″-H	5.99 (s, br, 4 H)	acetate CH_3:	4.54 (s, 6 H)
		β-H	7.20 (d, 2 H)		α″-H	0.29 (s, br, 4 H)		4.53 (s, 12 H)
		β′-H	5.99 (s, br, 2 H)		CH_3	2.83 (s, 6 H)		
		α′-H	0.29 (s, br, 2 H)					
		NH	7.41 (br, 1 H), 7.20 (1 H)					
		$NC_5H_4CH_2NH$	4.59 (d, 2 H), 4.30 (d, 2 H)					
		CH_2	2.85 (t, 2 H), 2.80 (t, 2 H), 2.53 (t, 2 H), 2.40 (t, 2 H)					
4a	C2PY	α-H	8.45 (d, 2 H)	MeIm:		6.21 (s, 2 H)	acetate CH_3:	4.92 (s, 6 H)
		β-H	7.21 (d, 2 H)			1.82 (s, 2 H)		3.44 (s, 12 H)
		β′-H	6.11 (s, br, 2 H)			*ca.* 2.8 (2 H)[a]		
		α′-H	−0.64 (s, br, 2 H)	CH_3		2.81 (s, 6 H)		
		NH	7.04 (t, br, 1 H), 6.71 (t, br, 1 H)					
		$NC_5H_4CH_2NH$	4.99 (d, 2 H), 4.32 (d, 2 H)					
		CH_2	2.88 (t, 2 H), 2.79 (t, 2 H), 2.52 (t, 2 H), 2.38 (t, 2 H)					
5b	C10PY:	α-H	8.46 (d, 2 H)	mpy:	β″-H	5.96 (s, 4 H)	acetate CH_3:	4.56 (s, 6 H)
		β-H	7.18 (d, 2 H)		α″-H	0.24 (s, 4 H)		4.54 (s, 12 H)
		β′-H	5.90 (s, br, 2 H)		CH_3	2.82 (s, 6 H)		
		α′-H	0.39 (s, br, 2 H)					
		NH	6.90 (s, br, 1 H), 6.57 (t, br, 1 H)					
		$NC_5H_4CH_2NH$	4.58 (d, 2 H), 4.30 (d, 2 H)					
		CH_2	2.70 (t, 4 H), 1.70–1.22 (m, 36 H)					

[a] Overlapping signal. The existence is deduced based upon the integral intensity of the overlapping resonances centred at *ca.* δ 2.8.

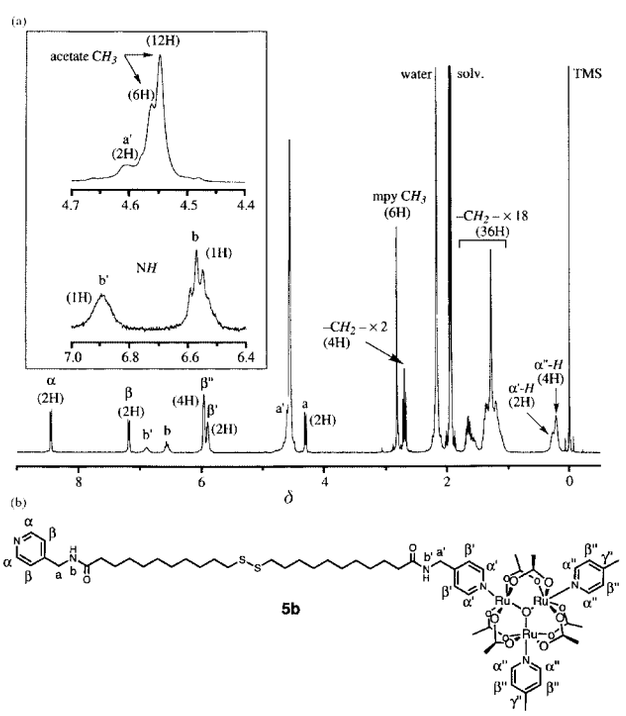

Fig. 2 (a) ^{1}H NMR spectrum of compound **5b** in CD_3CN at 20 °C. Inset: expanded spectra for the acetate methyl resonances (δ 4.4–4.7, upper) and for the NH resonances (δ 6.4–7.0, bottom). (b) Proton labeling scheme for **5b**.

7.18 (2 H) are ascribed to the α- and β-protons of the pyridyl ring in C10PY free from co-ordination, respectively; those are nearly identical to the chemical shift values of the corresponding signals for the free C10PY molecule in $CDCl_3$ (δ 8.54 and 7.17, respectively; the NMR spectroscopic data are given in the Experimental section). Indeed these two signals are coupled to each other in the ^{1}H–^{1}H COSY spectrum (not shown). Two singlets found at δ 5.96 (4 H) and 5.90 (2 H) are assigned to the paramagnetically upfield shifted[18–21] β″-protons (mpy) and β′-protons (of the co-ordinated pyridyl ring in C10PY), respectively. Owing to the same effect, signals of α″-protons (mpy) and α′-protons (C10PY) which are in a close proximity of ruthenium(III) centres are observed as broad singlets in further upfield, δ 0.24 (4 H) and 0.39 (2H), respectively. Two signals at δ 4.30 (doublet, 2 H) and 4.58 (2 H, overlapping with one of the acetate CH_3 signals; see later) can be ascribed to the methylene protons a and a′, respectively. Also the 1 : 1 split signals for the NH moieties are observable at δ 6.90 (broad singlet, 1 H) and 6.57 (broad triplet, 1 H) and are assigned to the protons b′ and b, respectively (see inset (bottom) in Fig. 2a). These assignments are supported by the COSY spectrum; the doublet signal a has cross-peaks with the aromatic β-proton signal and also with the NH triplet signal b, while the methylene resonance a′ has a cross-peak with the NH signal b′. Mixed terminal ligand stoichiometry in **5b**, *e.g.* two mpy ligands and one C10PY ligand, is evident from the appearance of two acetate CH_3 singlets in the 1 : 2 ratio at δ 4.56 and 4.54 (see inset (top) in Fig. 2a). Resonances of a total of 20 methylene groups in **5b** are found at δ 2.70 (corresponding to two methylene groups) and in the region between δ 1.70 and 1.22 (corresponding to 18 methylene groups). In the case of C2PY complexes **3a** and **4a**, six well resolved methylene resonances of the C2PY moiety are observed (Table 1).

UV-vis and infrared absorption spectroscopy

Absorption spectral data of the present complexes are summarized in Table 2. Triruthenium(III) compounds containing pyridine-based terminal ligands generally show three absorption

Table 2 Electronic absorption spectral data (CH_3CN)[a]

Complex	λ/nm (ε/dm^3 mol^{-1} cm^{-1})		
	IC[b]	CLCT[c]	π–π^*[d]
1b	697 (5900), 610 (sh, 4200)	390 (sh, 3100)	277 (18000), 233 (sh, 22000)
2a	683 (4500), 615 (sh, 3900)	380 (2600), 340 (sh, 3900)	275 (sh, 11300), 240 (sh, 15700)
3a	692 (6300), 610 (sh, 4600)	385 (sh, 3600), 335 (sh, 8600)	278 (19300), 237 (24800)
4a	679 (6500), 610 (sh, 5200)	335 (sh, 7800)	280 (sh, 15800), 240 (sh, 25600)
5b	691 (6600), 615 (sh, 4700)	375 (sh, 4000), 325 (sh, 10100)	279 (20000), 234 (26000)

[a] sh = Shoulder. [b] Intracluster "$Ru_3(\mu_3\text{-}O)$" transitions between molecular orbitals arising from dπ(Ru)–p$\pi(\mu_3$-O) interactions. [c] Cluster-to-ligand charge-transfer transitions. [d] π–π^* transitions in terminal ligands.

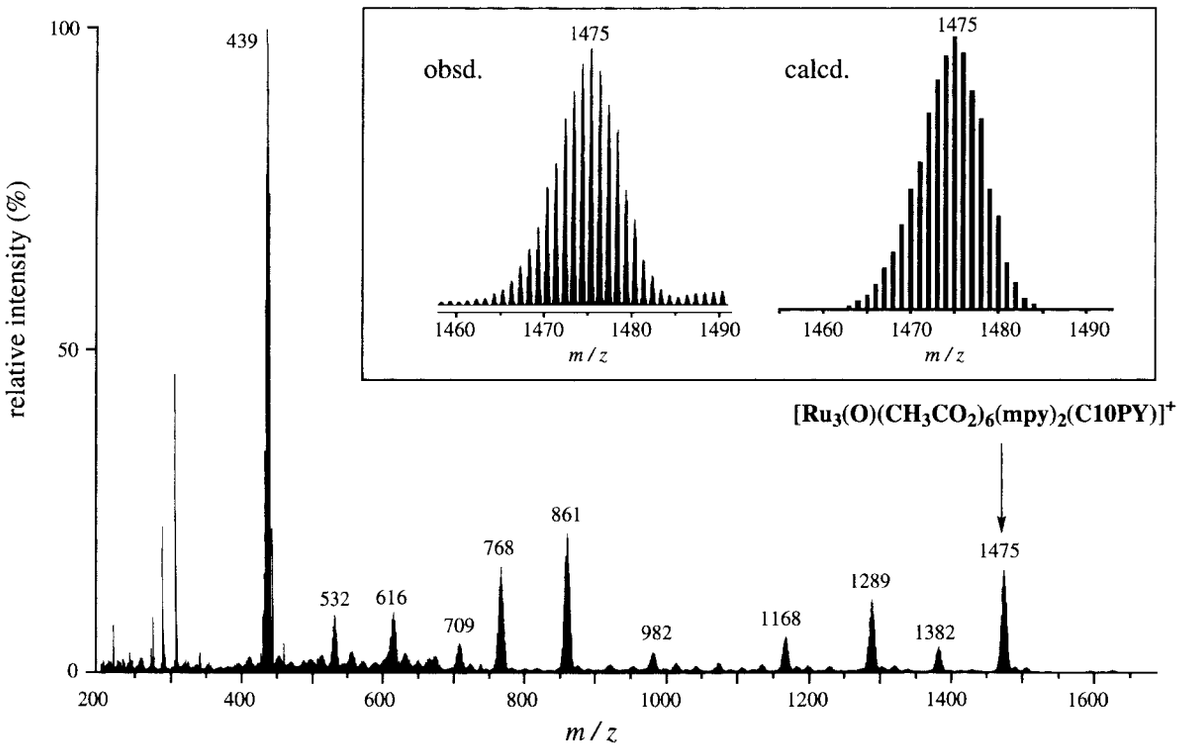

Fig. 3 A FAB mass spectrum of compound **5b** in the mass region between 200 and 1700. Inset: observed (left) and calculated (right) isotope patterns for the molecular ion of **5b**.

bands in the UV-vis region. On the basis of the spectral assignments described for the known analogues,[18–21] a broad absorption band centred at 679–697 nm with a shoulder at 610–615 nm is ascribed to the intracluster $\{Ru_3(O)\}$ charge-transfer (ICCT) transitions. Absorptions around 335–390 nm are assigned to the cluster-to-ligand charge-transfer (CLCT) transitions. The highest energy absorption bands are ascribed to the π–π^* transitions of aromatic rings in terminal ligands. The absorption spectral features are very similar within the series of bis(mpy) complexes (**1b**, **3a** and **5b**) and the series of bis(MeIm) complexes (**2a** and **4a**).

In the infrared spectra all the compounds display the acetate stretches with a broad and a sharp absorption in the region 1540–1560 and around 1430 cm^{-1}, respectively; the former corresponds to the asymmetric stretch [$\nu_{asym}(CO_2^-)$] and the latter the symmetric stretch [$\nu_{sym}(CO_2^-)$].[25a] The energy differences between these two bands [$\nu_{asym}(CO_2^-) - \nu_{sym}(CO_2^-)$] correspond to 110–126 cm^{-1} which fall into the range of values observed for bridging carboxylate ions in inorganic metal compounds.[25b]

Mass spectrometry

Structural identification of C2PY and C10PY compounds (**3a**, **4a** and **5b**) was also carried out using FAB mass spectrometry. A FAB mass spectrum of **5b** is presented in Fig. 3. The mass spectrum of compound **5b** contains the parent peak m/z = 1475 which corresponds to $[M - (CF_3SO_3^-)]^+$. As seen in the inset of Fig. 3, the observed isotope distribution of the parent mass envelope (left) is consistent with the calculated one (right). The broad spectral feature of the mass envelopes is ascribed to the isotope distribution of the Ru atom (^{96}Ru–^{104}Ru). Most of the dominant fragment peaks observed at m/z > 400 are assignable to species with successive loss of terminal ligands (mpy and C10PY) and bridging acetate anion(s). Identical spectral characteristics are observed for compounds **3a** and **4a** (see ESI).† For all the three compounds the mass fragments corresponding to species with loss of half of the dialkyl disulfide ligand (C2PY or C10PY) are detected (m/z = 963 for **3a**; 1032 for **4a**; 1168 and 982 for **5b**).

Electrochemistry of the triruthenium(III) complexes in acetonitrile

The redox properties of complexes **5a**,**b** were studied by cyclic voltammetry (CV). Fig. 4 shows a cyclic voltammogram of **5b** dissolved in 0.1 M [n-Bu_4N]PF_6–CH_3CN measured at a scan rate of 100 mV s^{-1}. Table 3 collects electrochemical data of all the compounds, including those of the ligand C2PY, for comparison.

As shown in Fig. 4, compound **5b** displays three one-electron redox waves at +0.98, −0.06, and −1.34 V *vs.* Ag–AgCl in the

Table 3 Electrochemical data (20 °C) of the disulfide-containing ligand (C2PY) and triruthenium(III) complexes $[Ru_3(O)(CH_3CO_2)_6(mpy)_2(H_2O)]ClO_4$ **1a**, $[Ru_3(O)(CH_3CO_2)_6(MeIm)_2(CH_3OH)]ClO_4$ **2a**, $[Ru_3(O)(CH_3CO_2)_6(mpy)_2(C2PY)]ClO_4$ **3a**, $[Ru_3(O)(CH_3CO_2)_6(MeIm)_2(C2PY)]ClO_4$ **4a** and $[Ru_3(O)(CH_3CO_2)_6(mpy)_2(C10PY)]CF_3SO_3$ **5b** in CH_3CN containing 0.1 M $[n\text{-}Bu_4N]PF_6$ as supporting electrolyte

	$E_{1/2}$[a]/V *vs.* Ag–AgCl (ΔE_p[b]/mV)					
Complex	IV,IV,III–IV,III,III	IV,III,III–III,III,III	III,III,III–II,III,III	II,III,III–II,II,III	II,II,III–II,II,II	Ligand centred
C2PY						+1.40,[c] −0.40,[c] −2.06[d]
1a	[e]	+1.08 (90)	+0.04 (70)	−1.25 (80)	−2.12[d]	
2a	+1.97 (120)	+1.00 (110)	−0.08 (100)	−1.51[d]	−2.10[f]	
3a	+1.48[c]	+1.00 (70)	−0.05 (70)	−1.34 (80)	−2.13[d]	+1.40,[g] −2.05[d]
4a	+1.64[c]	+0.93 (70)	−0.17 (70)	−1.57[d]	−2.18[d,h]	+1.44,[c] −2.18[d]
5b	+1.50[c]	+0.98 (60)	−0.06 (60)	−1.34 (60)	−2.11[d,h]	+1.33,[c] 2.11[d,h]

[a] Half-wave potential. [b] Peak-to-peak separation. [c] Anodic peak potential for irreversible process. [d] Cathodic peak potential for irreversible process. [e] Not observed. [f] DPV peak value. [g] Detected as a shoulder in CV. [h] Overlapping wave.

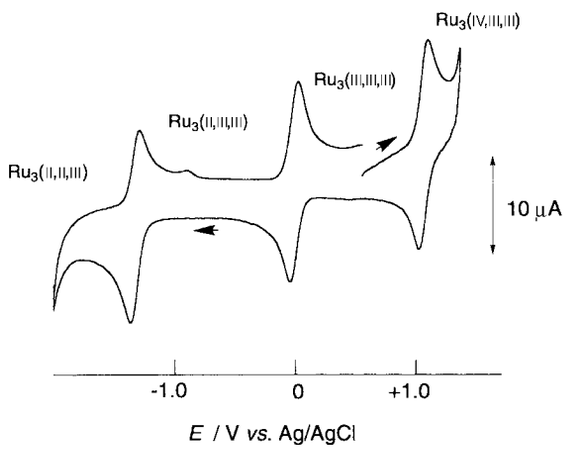

Fig. 4 Cyclic voltammogram of compound **5b** in CH_3CN containing 0.1 M $[n\text{-}Bu_4N]PF_6$ as a supporting electrolyte at 20 °C, a scan rate of 100 mV s^{-1}. The glassy carbon working electrode (diameter = 3 mm), a platinum wire counter electrode and an Ag–AgCl reference electrode are used.

applied potential range between +1.20 and –2.00 V. All these waves are ascribed to $\{Ru_3O\}$ core-based one-electron redox processes as established previously for related compounds.[19–21] Sequential redox processes of the compound generate four oxidation states, IV,III,III, III,III,III, II,III,III and II,II,III.

The three redox waves IV,III,III–III,III,III, III,III,III–II,III,III and II,III,III–II,II,III for all the compounds except **1a** and **2a** correspond to diffusion-controlled one-electron reversible processes according to the following observations: (i) the current peak intensity ratios of the cathodic and anodic waves (i_{pc} : i_{pa}) are close to unity; (ii) the peak-to-peak separation (ΔE_p) values are ≈60 mV, which do not depend on the scan rates (v = 20–500 mV s^{-1}); (iii) the current peak intensities correlate linearly with $v^{1/2}$. The replacement of the co-ordinated solvent in **1a**,**1b** and **2a** with the *N*-heterocyclic ligand C2PY or C10PY shifts the redox potentials negatively; this feature is evident by comparing the redox data of bis(mpy) compounds **1a**/**3a**, **1a**/**5a**, and those of the bis(MeIm) compounds **2a**/**4a** in Table 3. As discussed previously,[18–21] the $E_{1/2}$ values are dependent on the electronic character of the terminal *N*-heterocyclic ligands. Thus, the more electron-donating MeIm ligand (pK_a 7.3) pushes the redox potentials in the negative direction by 70–260 mV relative to the mpy ligand (pK_a 6.0). This feature is apparent by comparing redox potentials in the series **1a**/**2a** and **3a**/**4a**. The extent of the negative shift in the redox potentials (mpy ⟶ MeIm) becomes more significant for the processes found in the more negative potential region; for example, the difference in redox potentials in compounds **3a** and **4a** is 70 mV for the IV,III,III–III,III,III couple, while the difference increases to 120 mV for the III,III,III–II,III,III and 230 mV for the II,III,III–II,II,III couples. As seen in **3a**/**5b**, the chain length of the methylene groups of the disulfide ligands does not seem to modulate redox properties of the trimetallic centres.

In the most positive and negative potential regions the triruthenium centres and terminal dialkyl disulfide ligands are, in most cases, irreversibly oxidized or reduced. They are also included in Table 3. These assignments are based upon the comparison of the redox potentials for related Ru_3 species and those of the "free" ligand. The insoluble nature of C10PY in CH_3CN has precluded observation of the redox potentials of this ligand under identical conditions.

Electrochemistry of the monolayers

Preparation of the monolayer assembly of C10PY complex **5b** on a gold electrode, **5b**/Au, has been achieved in an identical manner to that for compounds **3a** and **4a** described previously,[13] and an idealized view of the monolayer is illustrated in the project Contents. Attachment of metal complexes on gold through alkyl- and amide-based ligands has been reported by other workers.[6k,8]

As shown in Fig. 5(a), the monolayers of **5b**/Au display a single redox wave in 0.1 M $NaClO_4$ (aq) (pH 7.0) in the applied potential range between +0.5 and −0.5 V. This wave is ascribed to the one-electron redox couple, III,III,III–II,III,III, based on the analogy of the redox potential and the reversibility found in the discrete molecule in acetonitrile (Table 3). It is confirmed that the CV of **5a**/Au (*i.e.*, the electrode derived from complex **5a**) is consistent with that of **5b**/Au.

CV of monolayers derived from the ligand C10PY shows no redox wave in the corresponding potential range. Integration of the voltammetric wave of **5b**/Au yields the surface coverage of the triruthenium redox centres, $\Gamma(Ru_3)$, to be 9.6×10^{13} cm^{-2}, which is approximately twice that of **3a**/Au, 4.4×10^{13} cm^{-2}. Since the molecular area of the trinuclear headgroup can be estimated to be ≈114 $Å^2$,[26] by assuming perpendicular orientation of the cluster to the gold surface, it is reasonable to conclude that close packing of the Ru_3 cluster moieties is achieved for monolayers **5b**/Au.

A plot of the current peak intensity of the anodic wave (i_{pa}) against the scan rate (v) is shown in Fig. 5(b). As expected for surface-confined redox centres, the i_{pa} values are directly proportional to v.[27] The value of the full width at half-maximum (W_{fwhm}) is 130 mV for the anodic wave, which exceeds the value of 90.6 mV expected for a one-electron redox process of surface-confined molecules with no lateral interactions.[28] The somewhat larger value observed for **5b**/Au suggests substantial repulsive interactions between the adjacent triruthenium redox centres.

Noteworthy is the significant stability of the monolayers toward repetitive potential cycles. For example, monolayers **5b**/Au showed no alternation in cyclic voltammograms during repeated potential scans (up to 1000 cycles at 100 mV s^{-1}) for the III,III,III–II,III,III process (−350 to +300 mV) at pH 7.0 in 0.1 M $NaClO_4$ aqueous solution. Furthermore, as far as the

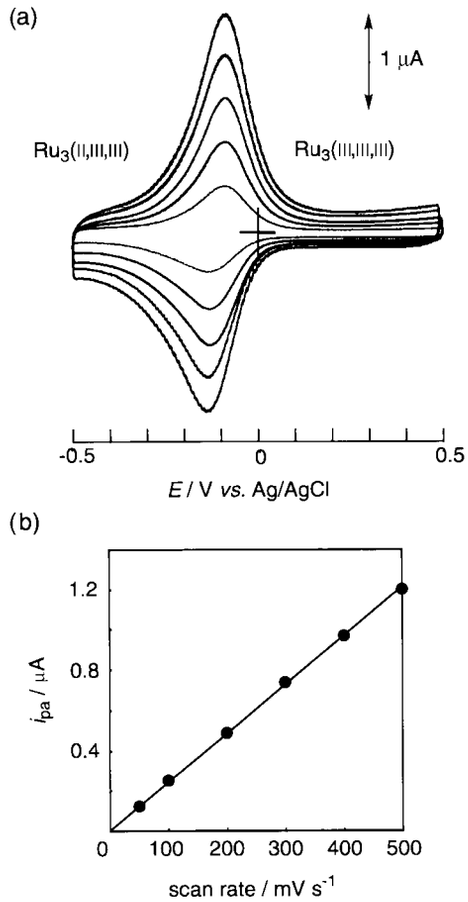

Fig. 5 (a) Cyclic voltammograms of monolayers of compound **5b** on a polycrystalline gold electrode, **5b**/Au, in 0.1 M $NaClO_4$ aqueous solution (pH 7.0) at 20 °C recorded at scan rates of 100, 200, 300, 400 and 500 mV s^{-1} (bottom to top). The surface coverage of Ru_3 redox centres is 9.6×10^{13} molecules cm^{-2}. A gold electrode with diameter 3.0 mm was used. The counter electrode and the reference electrode were a platinum wire and Ag–AgCl, respectively. (b) A plot of anodic current peak intensities against scan rates.

modified electrode was kept immersed in the ethanol solution containing complex **5b** (1 mM) at 20 °C, identical redox behaviour was observed during multiple electrochemical experiments (over two weeks). We speculate that the significant stability arises not only from the thermodynamic stability and kinetically inert character of the triruthenium(III) framework[29] but also from van der Waals interchain interactions among the surface-oriented C10PY ligands. Further, the surface structures may be stabilized by possible hydrogen-bonding interactions[30] between the neighboring amide groups in C10PY, as suggested for the C2PY system.[13]

An enhancement in the stability of the longer chain monolayers **5b**/Au relative to the shorter chain counterpart **3a**/Au is indicated by a reductive desorption experiment: in 0.5 M KOH (aq), a single reductive desorption wave for **5b**/Au is observed at −0.89 V, which is more negative compared to the corresponding value for **3a**/Au (−0.62 V) under identical conditions.[13]

Electrolyte effects

To confirm electrolyte effects upon voltammetric data, CV was performed using different types of sodium salts as supporting electrolytes ($NaClO_4$, $NaCF_3SO_3$, $NaNO_3$, $NaPF_6$ and Na_2SO_4). Complex **5b** is positively charged (+1) and it becomes neutral upon one-electron reduction. Thus, the Ru^{III}_3 headgroups in the monolayers require an equivalent amount of anions to compensate the electric charge, which will be released upon one-electron reduction of the cluster heads. It has been established for ferrocene-based self-assembled monolayers[31,32] that the formation constant for forming ion pairs between ferrocenium and anions determines the redox potential of the monolayers.

Table 4 Anion dependence of redox waves of monolayers (a) **3a**/Au and (b) **5b**/Au in water containing a 0.1 M supporting electrolyte[a]

Supporting Electrolyte[b]	$E_{1/2}$[c]/V	ΔE_p[d]/mV	W_{fwhm}(a)[e]/mV	W_{fwhm}(c)[f]/mV
(a) **3a**/Au[g]				
$NaPF_6$[h]	−0.110	35	150	150
$NaClO_4$	−0.095	30	160	160
$NaCF_3SO_3$	−0.095	30	185	190
Na_2SO_4	−0.090	30	250	245
$NaNO_3$	−0.085	20	230	230
(b) **5b**/Au[i]				
$NaPF_6$[h]	−0.130	20	135	135
$NaClO_4$	−0.100	20	130	140
$NaCF_3SO_3$	−0.100	30	120	120
Na_2SO_4	−0.060	20	200	210
$NaNO_3$	−0.020	50	200	220

[a] pH 7.0 (phosphate buffer). Potentials are reported with respect to Ag–AgCl at a scan rate of 500 mV s^{-1}. [b] The concentration of the supporting electrolytes was 0.10 M. [c] Half-wave potential. [d] Peak-to-peak separation. [e] Full width at half-maximum evaluated from the anodic wave. [f] Full width at half-maximum evaluated from the cathodic wave. [g] The surface coverage was 4.4×10^{13} Ru_3 molecules cm^{-2}. [h] Data obtained at pH 6.0. [i] The surface coverage was 9.6×10^{13} molecules cm^{-2}.

The anion dependence of the redox waves of monolayers **3a**/Au and **5b**/Au is compared in Table 4. The concentrations of the supporting electrolytes were fixed at 0.10 M and the solution pH is adjusted to 7.0 by use of Britton–Robinson buffer solution. It is found that the almost symmetrical feature of the redox wave, as seen in Fig. 5(a), is maintained for each electrolyte solution, except for the case of Na_2SO_4 (see above), but the redox potential is highly dependent on the type of anion. For both monolayers, the redox potentials shift in the negative direction in the order $SO_4^{2-} < NO_3^- < CF_3SO_3^- \approx ClO_4^- < PF_6^-$, indicating that the formation constant for ion pairs between the monopositive Ru_3 groups and anions becomes larger in this order.[31] The observed anion dependency is in good agreement with the trend seen for ferrocene-modified electrodes.[31–33] Interestingly, the observed anion effect seems more significant for longer alkyl chain monolayers **5b**/Au ($\Delta E_{1/2}$ = 110 mV) than the shorter chain counterpart **3a**/Au ($\Delta E_{1/2}$ = 25 mV). This pobably reflects the morphological variation in two monolayers and/or the local environments of the Ru_3 redox centres seen between the two, resulting from the chain length alternation of the adsorbed molecules along with the coverage density of the Ru_3 molecules (see below).

The full width at half-maximum (W_{fwhm}) values are also influenced by the anions; for monolayer **3a**/Au they range from 150 to 185 mV (cathodic waves) for $NaPF_6$, $NaClO_4$ and $NaCF_3SO_3$ solutions, while they become larger (from 230 to 250 mV) for Na_2SO_4 and $NaNO_3$ solutions. One of the reasons may be the occurrence of morphological disorder of the monolayers, induced by specific interactions of the last two anions.

The unusual redox response observed for monolayers **5b**/Au in the presence of SO_4^{2-} is also evident from the voltammetric shape, as shown in Fig. 6. Note that, since the pK_{a2} value of H_2SO_4 is 1.92,[34] the predominant anionic species due to the electrolyte is SO_4^{2-} under the present experimental conditions (pH > 2). As can be seen, the cathodic broad wave consists of a peak at −0.05 V with an apparent shoulder at *ca.* −0.2 V, and the cathodic and anodic traces are *not* identical. This unsymmetrical character is seen specifically for the Na_2SO_4 electrolyte solution, suggesting that SO_4^{2-} substantially influences the monolayer morphology and subsequent electron-transfer

Table 5 pH Dependence of the redox wave of III,III,III–II,III,III process for monolayers (a) **3a**/Au and (b) **5b**/Au in 0.1 M $NaClO_4$ aqueous solution [a]

(a) **3a**/Au					
pH	2.2	4.8	6.1	7.0	9.4
$E_{1/2}$ [b]/V	−0.070	−0.080	−0.077	−0.110	−0.090
ΔE_p/mV	15	20	25	20	30
W_{fwhm} [c]/mV	130	130	150	160	170
W_{fwhm} [d]/mV	130	140	140	170	170
(b) **5b**/Au					
pH	2.3	4.7	6.0	7.2	10.0
$E_{1/2}$ [b]/V	−0.070	−0.080	−0.080	−0.090	−0.100
ΔE_p/mV	30	30	30	40	60
W_{fwhm}(a) [c]/mV	130	130	140	130	130
W_{fwhm}(c) [d]/mV	130	140	140	140	140

[a] In water containing 0.10 M $NaClO_4$ as supporting electrolyte and Britton–Robinson buffer solution. [b] Redox potentials are quoted *vs.* Ag–AgCl. [c] Full width at half-maximum evaluated from the anodic wave. [d] Full width at half-maximum evaluated from the cathodic wave.

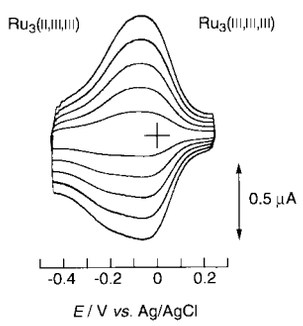

Fig. 6 CV of monolayers of compound **5b** on a polycrystalline gold electrode, **5b**/Au, in 0.1 M Na_2SO_4 aqueous solution (pH 7.0) at 20 °C recorded at scan rates of 100, 200, 300, 400 and 500 mV s^{-1} (bottom to top). Experimental conditions as in Fig. 5.

events between the Ru_3 centres and the electrode. Importantly, the voltammogram presented in Fig. 5(a) (0.1 M $NaClO_4$, pH 7.0) can completely be reproduced using the same electrode upon substitution of the electrolyte solution by 0.1 M Na_2SO_4 (aq). The reproducibility of these two electrolytes was also confirmed at pH 4.5.

pH Dependence

Redox properties of monolayers **3a**/Au and **5b**/Au were examined in a wide pH range with the use of 0.1 M $NaClO_4$ (aq). The electrochemical data are summarized in Table 5. Although the Ru_3 redox centres have no protonation/deprotonation site, there are equivalent amounts of pyridyl residues in the monolayers, and protonation may be possible in acidic media to generate positively charged pyridinium groups. Beulen *et al.*[35] have reported that for mixed monolayers consisting of both ferrocene redox centres and carboxylic acid residues the observed ferrocene–ferrocenium redox wave was dramatically altered by the protonation/deprotonation behaviour of the neighboring carboxylates. In the present system, however, almost identical cyclic voltammograms are observed at pH 2.3–10.0, with a small deviation of $E_{1/2}$, ΔE_p and W_{fwhm}, indicating that neither Ru_3 monolayer structures nor electron-transfer rates are largely affected by solution pH. The CV variation is too small to assess the possible protonation/deprotonation equilibrium at the nitrogen sites of the unco-ordinated pyridyl rings.

Conclusion

This work demonstrates tunable redox properties of redox-active (μ_3-oxo)triruthenium(III) complexes self-assembled onto gold electrode surfaces. The triruthenium complexes with the disulfide ligands **3a**–**5b** were characterized by spectroscopic and electrochemical methods. An anion-dependent nature of the one-electron reversible redox process found in the surface system can be rationalized by the difference in degree of interaction between the positively charged Ru^{III}_3 centres and the electrolyte anions in solution, and the trend of the redox potential with various anions is similar to the electrochemical behaviour found in metal complex-modified electrodes.

Experimental

Materials

Reagents and solvents used were of commercially available reagent-grade quality unless otherwise stated. $RuCl_3 \cdot 3H_2O$ was purchased from Shiga Kikinzoku Co. Acetonitrile used for electrochemical measurements was distilled from CaH_2 under argon. Tetrahydrofuran (THF) was distilled from sodium–benzophenone under Ar. Silica gel (Wako C–300, Wako Chemicals) was used for column chromatography. Ultrapure water was obtained by using a Milli-Q water purification system (Yamato, WQ–500). A gold disk (Ishihuku Metal, 99.99%; diameter 10 mm, thickness 3 mm) and a glass (Matsunami Glass, 20 × 26 mm) was used for Au(111) substrates. Ultrapure N_2 (99.99%) and Ar (99.95%) (Daido Hokusan) were used.

Physical methods

Infrared spectra were recorded on a Hitachi 270–50 infrared spectrophotometer using KBr disks, electronic absorption spectra by a Hitachi U–3410 spectrophotometer, ^1H and ^{13}C-{^1H} NMR spectra on a JEOL JNM–EX 270 NMR spectrometer at 270.15 and 67.94 MHz, respectively. All chemical shifts are reported as δ values downfield from an internal standard of tetramethylsilane (TMS). Fast atom bombardment (FAB) mass spectra were recorded on a JEOL JMS-HX110 mass spectrometer at the Center for Instrumental Analysis, Hokkaido University in the positive-ion mode with 3-nitrobenzyl alcohol as matrix.

Electrochemistry of triruthenium complexes in acetonitrile

Cyclic voltammetry was performed using a BAS CV-50W voltammetric analyzer with Hokuto HA-501G potentiostat and a HB-105 function generator equipped with a Graphtec WX2400 X-Y recorder. The working electrode, the auxiliary electrode, and a reference electrode were glassy carbon, platinum coil, and Ag–AgCl, respectively. Differential-pulse voltammetry (DPV) was carried out by the same equipment at a scan rate of 20 mV s^{-1}. The electrochemical measurements were achieved at room temperature under an argon atmosphere in acetonitrile solution containing 0.10 M tetrabutylammonium hexafluorophosphate, [*n*-Bu_4N]PF_6, with a complex concentration of 0.5–1.0 mM. Under these conditions the half-wave potential ($E_{1/2}$) of the ferrocene–ferrocenium couple (Fc–Fc^+) was observed at +0.435 V *vs.* Ag–AgCl with a peak-to-peak separation (ΔE_p) of 60 mV at a scan rate of 100 mV s^{-1}.

Syntheses

The triruthenium(III) complexes $[Ru_3(O)(CH_3CO_2)_6(mpy)_2(CO)]$ (mpy = 4-methylpyridine), $[Ru_3(O)(CH_3CO_2)_6(MeIm)_2(CO)]$ (MeIm = 1-methylimidazole), $[Ru_3(O)(CH_3CO_2)_6(mpy)_2(H_2O)]ClO_4$ **1a**, $[Ru_3(O)(CH_3CO_2)_6(MeIm)_2(CH_3OH)]ClO_4$ **2a**, $[Ru_3(O)(CH_3CO_2)_6(mpy)_2(C2PY)]ClO_4$ **3a** and $[Ru_3(O)(CH_3CO_2)_6(MeIm)_2(C2PY)]ClO_4$ **4a**, were prepared as described previously.[13] The ligand C2PY was prepared according to the literature procedures.[8] ^{13}C-{^1H} NMR (solvent $CDCl_3$; standard $SiMe_4$; 20 °C): δ_C 171.06 (C=O), 149.58 (py α-C), 147.10 (py γ-C), 122.11 (py β-C), 42.73 ($NC_5H_4CH_2$), 35.42, 34.01 (CH_2).

$CH_3C(O)S(CH_2)_{10}C(O)NHCH_2C_5H_4N$ (Ac-S-C10-py). The acid $CH_3C(O)S(CH_2)_{10}CO_2H$ (2.61 g, 10.0 mmol)[36] and 1,1′-carbonyldiimidazole (1.78 g, 11 mmol) were dissolved in THF (45 cm^3). To this was added dropwise argon-purged 4-(aminomethyl)pyridine (1.1 cm^3, 11 mmol), and the mixture stirred for 24 h under argon. The reaction was monitored by TLC; after 24 h a single spot ($R_f = 0.69$) was obtained for the reaction mixture (eluted with CH_3OH), the value being different from that of starting materials $CH_3C(O)S(CH_2)_{10}CO_2H$ ($R_f = 1.0$) and 4-(aminomethyl)pyridine ($R_f = 0.28$) under the same conditions. An oily product (*ca.* 5 cm^3) was obtained by reducing the solvent on a rotary evaporator (the temperature was maintained at 32–42 °C during this procedure) and dissolved in CH_3OH (4 cm^3). The addition of diethyl ether (25 cm^3) and storage of the mixture at 0 °C for 3 weeks resulted in the precipitation of a white solid, which was collected by filtration, washed with diethyl ether (5 $cm^3 \times 4$) and dried under vacuum (1.65 g, 47%) (Found: C, 64.79; H, 8.68; N, 8.30; S, 8.92. $C_{19}H_{30}N_2O_2S$ requires C, 65.11; H, 8.63; N, 7.99; S, 9.15%); δ_H(solvent $CDCl_3$; standard $SiMe_4$; 20 °C) 8.51 (2 H, d, py α-H), 7.17 (2 H, d, py β-H), 6.50 (1 H, m, NH), 4.23 (2 H, d, NC_5H_4-CH_2N), 2.85 (2 H, t, CH_2), 2.32 (3 H, s, CH_3CO), 2.26 (2 H, t, CH_2), 1.66–1.56 (4 H, m, CH_2) and 1.27 (12 H, br s, CH_2); δ_C($CDCl_3$) 195.93 (CH_3C=O), 173.28 (NHC=O), 149.42 (py α-C), 147.72 (py γ-C), 122.07 (py β-C), 42.09 ($NC_5H_4CH_2NH$), 36.45, 30.60, 29.39, 29.27 (an overlapping signal), 29.20, 29.18, 29.04, 28.95, 28.67 ($CH_2 \times 10$) and 25.66 (CH_3C=O); $\tilde{\nu}_{max}/cm^{-1}$ (KBr disk) 3296, 3080 (aromatic C–H), 2924, 2852, 1696 (CH_3C=O), 1652 (NHC=O) and 1545 (aromatic C–C, py).

$\{(NC_5H_4)CH_2NHC(O)(CH_2)_{10}S\}_2$ C10PY. A 1.24 g (3.54 mmol) amount of Ac-S-C10-py was dissolved in CH_3OH (50 cm^3) and a 0.55 g (3.98 mmol) K_2CO_3 added. The mixture was stirred at room temperature for 43 h and the solvent removed by a rotary evaporator. The oily product thus obtained was dissolved in CH_3OH (16 cm^3) by warming with a hot water bath. A white solid was obtained from the yellow solution by cooling and keeping at room temperature for 2 d. It was collected by filtration, washed with diethyl ether (40 cm^3), and dried under vacuum (575 mg, 53%), TLC $R_f = 0.92$ (CH_3OH) (Found: C, 64.86; H, 8.80; N, 8.68; S, 10.03. $C_{34}H_{54}N_4O_2S_2 \cdot CH_3OH$ requires C, 64.98; H, 9.04; N, 8.66; S, 9.91%); δ_H($CDCl_3$) 8.54 (4 H, d, py α-H), 7.17 (4 H, d, py β-H), 6.09 (2 H, br t, NH), 4.44 (4 H, d, $NC_5H_4CH_2N$), 2.68 (4 H, t, CH_2), 2.26 (4 H, t, CH_2), 1.68 (8 H, m, CH_2) and 1.29 (30 H, br s, CH_2 + water); δ_C($CDCl_3$) 173.04 (C=O), 149.74 (py α-C), 147.29 (py γ-C), 122.03 (py β-C), 42.17 ($NC_5H_4CH_2NH$), 42.2, 39.1, 36.6, 29.4, 29.3, 29.3 (an overlapping signal), 29.1, 29.1, 28.4 ($CH_2 \times 10$); $\tilde{\nu}_{max}/cm^{-1}$ (KBr disk) 3300, 3076 (aromatic C–H), 2920 (CH_2), 2848 (CH_2), 1644 (NHC–O), 1554 (C–C, pyridyl) and 802 (N–H); *m*/*z* (EI) 614 (M^+).

$[Ru_3(O)(CH_3CO_2)_6(mpy)_2(CH_3OH)]CF_3SO_3$ 1b. $[Ru_3(O)(CH_3CO_2)_6(CO)(mpy)_2]$ (4.45 g, 0.504 mmol) was dissolved in CH_3OH (25 cm^3)–CH_2Cl_2 (30 cm^3) at room temperature. A CH_3OH solution (6 cm^3) containing $AgCF_3SO_3$ (270 mg, 1.05 mmol) was added and the mixture stirred in the dark for 24 h. The resultant solution was filtered through Celite. Addition of the filtrate to vigorously stirred diethyl ether (1000 cm^3) resulted in precipitation of complex **1b**, which was collected by filtration, washed with *n*-pentane (10 $cm^3 \times 3$) and dried under vacuum (469 mg, 69%) {Found: C, 25.07; H, 3.05; N, 2.14; S, 4.82. $[Ru_3(O)(CH_3CO_2)_6(mpy)_2(CH_3OH)]CF_3SO_3 \cdot CH_3OH \cdot AgCF_3SO_3$ ($C_{28}H_{40}AgF_6N_2O_{21}Ru_3S_2$) requires C, 25.29; H, 3.03; N, 2.11; S, 4.82%}; $\tilde{\nu}_{max}/cm^{-1}$ (KBr) 1556m,br {$\nu_{asym}(CO_2^-$, acetate)}, 1430vs {$\nu_{sym}(CO_2^-$, acetate)}, 1258s, 1162m, 1034m ($CF_3SO_3^-$).

$[Ru_3(O)(CH_3CO_2)_6(mpy)_2(C10PY)_2]ClO_4$ 5a. This complex was prepared in the identical manner for **5b** described below, except that **1a** and $NaClO_4$ were used in place of **1b** and $NaCF_3SO_3$ (8 mg, 14%) {Found: C, 42.90; H, 5.27; N, 5.27; S, 5.97. $[Ru_3(O)(CH_3CO_2)_6(mpy)_2(ClOPY)]ClO_4 \cdot 2H_2O$ ($C_{58}H_{86}ClN_6O_{19}Ru_3S_2$) requires C, 43.16; H, 5.40; N, 5.12; S, 5.86%).

$[Ru_3(O)(CH_3CO_2)_6(mpy)_2(C10PY)_2]CF_3SO_3$ 5b. Under an argon atmosphere, compound **1b** (289 mg, 0.215 mmol) and C10PY (516 mg, 0.839 mmol) were dissolved in CH_3OH (30 cm^3)–CH_2Cl_2 (60 cm^3) and the solution was stirred at room temperature for 124 h. As the reaction proceeded the electronic absorption peak at 679 nm for the original solution shifted to 691 nm in 100 h and remained unchanged afterwards. After 124 h the deep blue solution was evaporated to dryness by a rotary evaporator. The resultant crude solid was purified by column chromatography using a silica gel column (2.5 cm diameter × 20 cm long) and a 10% CH_3OH–CH_2Cl_2 solution as eluant. The major fraction, deep blue, was collected and the solvent removed. The crude solid was dissolved in CH_3OH (3 cm^3) containing $NaCF_3SO_3$ (44 mg, 0.256 mmol). The addition of diethyl ether (35 cm^3) and subsequent cooling at 0 °C for 16 h resulted in the precipitation of a solid product **5b**, which was collected by filtration, washed with diethyl ether (15 cm^3) and water (25 cm^3) and dried under vacuum (129 mg, 29%) {Found: C, 42.90; H, 5.27; N, 5.27; S, 5.97. $[Ru_3(O)(CH_3CO_2)_6(mpy)_2(C10PY)_2]CF_3SO_3 \cdot H_2O$ ($C_{59}H_{88}F_3N_6O_{19}Ru_3S_3$) requires C, 43.16; H, 5.40; N, 5.12; S, 5.86%}; $\tilde{\nu}_{max}/cm^{-1}$ (KBr disk) 1624m {ν(CO, C10PY)}, 1542m,br {$\nu_{asym}(CO_2^-$, acetate)}, 1432vs {$\nu_{sym}(CO_2^-$, acetate)}, 1270s, 1154m, 1034m ($CF_3SO_3^-$).

Electrode surface modifications with triruthenium(III) complexes

Self-assembly of compound **5b** on gold electrodes was conducted in an identical manner to the case of monolayers of compounds **3a** and **4a** on Au(111) as described previously.[13]

Electrochemistry of the monolayers on gold electrodes

The gold electrodes (diameter, 3.0 mm) with (111) ordered surface structures were prepared according to the method previously described[37,38] and used for subsequent surface modifications with the molecular adsorbates. The roughness factor of the surface was estimated to be less than 1.2 based on the observed charge for the reduction of gold oxide. Prior to the surface modification, the electrodes were washed with pure water, annealed in a hydrogen flame, and quenched with pure water.

The self-assembled monolayers of the triruthenium(III) complexes on gold were prepared by immersing the gold electrodes in ethanolic solutions containing 1.0 mM of the appropriate complex for 14 days. Prior to the electrochemical measurements, the modified gold electrodes were washed with ethanol and water, and then sonicated for 1 min in Milli-Q water to remove any possible physisorbed materials. It was found that upon the sonification procedure 5–10% of Ru_3 complex-derived species were eliminated from gold surfaces (estimated from an observed decrease in the area of the voltammetric wave).

The modified gold electrodes were placed in an electrode holder made from Kel-F so that only one face of the substrate touched an electrolyte solution meniscus. A platinum wire and an Ag–AgCl (sat. NaCl) were used as counter and reference electrodes, respectively. The pH of the solution was adjusted by using Mellvaine buffer solution (pH 2–8) containing 0.1 M $NaClO_4$ as an electrolyte or $HClO_4$ (pH 1.0). The electrolyte solution was deaerated by bubbling pure N_2 gas for 30 min prior to electrochemical measurements. The electrode potential was controlled by using a potentiostat (Hokuto Denko, HA-301) and external potential was provided by using a function generator (Hokuto Denko, HB-115). Cyclic voltammograms were recorded on an X-Y recorder (Rika Denki, RW-11T). All the measurements were carried out at room

temperature. Potentials in this paper are all presented with respect to Ag–AgCl (sat. NaCl).

CAUTION: perchlorate salts of metal complexes with organic ligands are potentially explosive.[39] Only small amounts of material should be prepared, and handled with great caution.

Acknowledgments

This work was supported by Grant-in-Aids for Scientific Research on Priority Area "Electrochemistry of Ordered Interfaces" (Nos. 09554037 and 09237106), and No. 09740483 from the Ministry of Education, Science, Sports, and Culture, Japan.

References

1 For example: J.-M. Lehn, *Science*, 1993, **260**, 1762.

2 A. Ulman, *An Introduction to Ultrathin Organic Films from Langmuir-Blogett to Self-Assembly*, Academic Press, New York, 1991; C. D. Bain and G. M. Whitesides, *Angew. Chem., Int. Ed. Engl.*, 1989, **28**, 506; G. M. Whitesides and P. E. Laibinis, *Langmuir*, 1990, **6**, 87; L. H. Dubois and R. G. Nuzzo, *Annu. Rev. Phys. Chem.*, 1992, **43**, 437; A. Ulman, *Chem. Rev.*, 1996, **96**, 1533; A. E. Kaifer, *Prog. Colloid Polym. Sci.*, 1997, **103**, 193; I. Wilner, *Acc. Chem. Res.*, 1997, **30**, 357; R. M. Crooks and A. J. Ricco, *Acc. Chem. Res.*, 1998, **31**, 219.

3 Selected references: C. E. D. Chidsey, C. R. Bertozzi, T. M. Putvinski and A. M. Mujsce, *J. Am. Chem. Soc.*, 1990, 112, 4301; C. E. D. Chidsey, *Science*, 1991, **251**, 919; J. J. Hickman, D. Ofer, P. E. Laibinis, G. M. Whitesides and M. S. Wrighton, *Science*, 1991, **252**, 688; J. J. Hickman, D. Ofer, C. Zou, M. S. Wrighton, P. E. Laibinis and G. M. Whitesides, *J. Am. Chem. Soc.*, 1991, **113**, 1128; D. M. Collard and M. A. Fox, *Langmuir*, 1991, **7**, 1192; H. C. DeLong, J. J. Donohue and D. A. Buttry, *Langmuir*, 1991, **7**, 2196; J. N. Richardson, S. R. Peck, L. S. Curtin, L. M. Tender, R. H. Terrill, M. T. Carter, R. W. Murray, G. K. Rowe and S. E. Creager, *J. Phys. Chem.*, 1995, **99**, 766; B. R. Herr and C. A. Mirkin, *J. Am. Chem. Soc.*, 1994, **116**, 1157; D. J. Campbell, B. R. Herr, J. C. Hulteen, R. P. Van Duyne and C. A. Mirkin, *J. Am. Chem. Soc.*, 1996, **118**, 10211; M. Maskus and H. D. Abruña, *Langmuir*, 1996, **12**, 4455; K. Chen, F. Xu and C. Mirkin, *Langmuir*, 1996, **12**, 2622; G. K. Kane and P. E. Laibinis, *J. Am. Chem. Soc.*, 1997, **119**, 5208; K. Weber, L. Hockett and S. Creager, *J. Phys. Chem. B.*, 1997, **101**, 8286.

4 K. Uosaki, Y. Sato and H. Kita, *Langmuir*, 1991, **7**, 1510; *Langmuir*, 1991, **7**, 1170; K, Shimazu, I. Yagi, Y. Sato and K. Uosaki, *J. Electroanal. Chem. Interfacial Chem.*, 1994, **372**, 117; K. Uosaki, Y. Sato and H. Kita, *Electrochim. Acta*, 1991, **36**, 1799; Y. Sato, H. Itoigawa and K. Uosaki, *Bull. Chem. Soc. Jpn.*, 1993, **66**, 1032; K. Kondo, S. Horiuchi, I. Yagi, S. Ye and K. Uosaki, *J. Am. Chem. Soc.*, 1999, **121**, 7155.

5 J. Zak, H. Yuan, K. Ho, L. K. Woo and M. D. Porter, *Langmuir*, 1993, **9**, 2772; J. E. Hutchison, T. A. Postlethwaite and R. W. Murray, *Langmuir*, 1993, **9**, 3277; A. Kay, R. Hamphry-Baker and M. Gratzel, *J. Phys. Chem.*, 1994, **98**, 952; L. H. Guo, G. McLendon, H. Razafitrimo and Y. Gao, *J. Mater. Chem.*, 1996, **6**, 369; K. Shimazu, M. Takechi, H. Fujii, M. Suzuki, H. Saiki, T. Yoshimura and K. Uosaki, *Thin Solid Films*, 1996, **273**, 250; J. Wienke, F. Kleima, R. Koehorst and T. Schaafsma, *Thin Sold Films*, 1996, **279**, 87; J. P. Collman, M. S. Ennis, D. A. Offord, L. L. Chng and J. H. Griffin, *Inorg. Chem.*, 1996, **35**, 1751; D. A. Offord, S. B. Sachs, M. S. Ennis, T. A. Eberspacher, J. H. Griffin, C. E. D. Chidsey and J. P. Collman, *J. Am. Chem. Soc.*, 1998, **120**, 4478; G. Ashkenasy, G. Kalyuzhny, J. Libman, I. Rubinstein and A. Shanzer, *Angew. Chem., Int. Ed.*, 1999, **38**, 1257; N. Kanayama, T. Kanbara and H. Kitano, *J. Phys. Chem. B.*, 2000, **104**, 271.

6 (*a*) H. O. Finklea, D. A. Snider and J. Fedyk, *Langmuir*, 1990, **6**, 371; (*b*) S. Y. Obeng and A. J. Bard, *Langmuir*, 1991, **7**, 195; (*c*) H. O. Finklea and D. D. Hanshew, *J. Am. Chem. Soc.*, 1992, **114**, 3173; (*d*) H. O. Finklea and D. D. Hanshew, *J. Electroanal. Chem. Interfacial Electrochem.*, 1993, **347**, 327; (*e*) H. O. Finklea, M. S. Ravenscroft and D. A. Snider, *Langmuir*, 1993, **9**, 223; (*f*) J. Redepenning, H. M. Tunison and H. O. Finklea, *Langmuir*, 1993, **9**, 1404; (*g*) M. S. Ravenscroft and H. O. Finklea, *J. Phys. Chem.*, 1994, **98**, 3843; (*h*) S. Yamada, H. Kohrogi and T. Matsuo, *Chem. Lett.*, 1995, 639; (*i*) Y. Sato and K. Uosaki, *J. Electroanal. Chem. Interfacial Chem.*, 1995, **384**, 57; (*j*) H. V. Ryswyk, E. D. Turtle, R. Watson-Clark, T. A. Tanzer, T. K. Herman, P. Y. Chong, P. J. Waller, A. L. Taurog and C. E. Wagner, *Langmuir*, 1996, **12**, 6143; (*k*) J. Luo and S. S. Isied, *Langmuir*, 1998, **14**, 3602; (*l*) I. C. N. Diógenes, F. C. Nart and I. S. Moreita, *Inorg. Chem.*, 1999, **38**, 1646; (*m*) C. A. Panetta, H. J. Kumpaty, N. E. Heimer, M. C. Leavy and C. L. Hussey, *J. Org. Chem.*, 1999, **64**, 1015.

7 D. Acevedo and H. D. Abruña, *J. Phys. Chem.*, 1991, **95**, 9590; R. J. Forster and L. R. Faulkner, *J. Am. Chem. Soc.*, 1994, **116**, 5444; R. J. Forster, *Inorg. Chem.*, 1996, **35**, 3394.

8 T. T. Ehler, N. Malmberg, K. Carron, B. P. Sullivan and L. J. Noe, *J. Phys. Chem. B*, 1997, **101**, 3174.

9 G. M. Ferrence, J. I. Henderson, D. G. Kurth, D. A. Morgenstern, T. Bein and C. P. Kubiak, *Langmuir*, 1996, **12**, 3075.

10 B.-H. Huisman, H. Schönherr, W. T. S. Huck, A. Friggeri, H.-J. van Manen, E. Menozzi, G. J. Vancso, F. C. J. M. van Veggel and D. N. Reinhoudt, *Angew. Chem., Int. Ed.*, 1999, **38**, 2248.

11 T. Inomata, M. Abe, T. Kondo, K. Umakoshi, K. Uosaki and Y. Sasaki, *Chem. Lett.*, 1999, 1097.

12 Y. Sasaki, T. Inomata, M. Abe, T. Kondo and K. Uosaki, The Electrochemical Society, 1999 Joint International Meeting, Honolulu, October 17–22, 1999, Abstract No. 2204; H. Takagi, A. Ichimura, T. Yano, I. Kinoshita, K. Isobe, M. Abe, Y. Sasaki, Y. Mikata, T. Tanase, N. Takeshita, C. Inoue, Y. Kimura, S. Endo, K. Tamura and S Yano, *Electrochemistry*, 1999, **67**, 1192.

13 M. Abe, T. Kondo, K. Uosaki and Y. Sasaki, *J. Electroanal. Chem. Interfacial Electrochem.*, 1999, **473**, 93.

14 M. Abe, S. Ye, T. Kondo, K. Uosaki and Y. Sasaki, *Electrochemistry*, 1999, **67**, 1162.

15 M. Valli, S. Miyata, H. Wakita, T. Yamaguchi, A. Kikuchi, K. Umakoshi, T. Imamura and Y. Sasaki, *Inorg. Chem.*, 1997, **36**, 4622; A. Kikuchi, T. Fukumoto, K. Umakoshi, Y. Sasaki and A. Ichimura, *J. Chem. Soc., Chem. Commun.*, 1995, 2125; T. Imamura, A. Kishimoto, T. Sumiyoshi, K. Takahashi and Y. Sasaki, *Bull. Chem. Soc. Jpn.*, 1995, **68**, 3365; Y. Sasaki, K. Umakoshi, T. Imamura, A. Kikuchi and A. Kishimoto, *Pure Appl. Chem.*, 1997, **69**, 205; T. Fukumoto, A. Kikuchi, K. Umakoshi and Y. Sasaki, *Inorg. Chim. Acta*, 1998, **283**, 151.

16 R. D. Cannon and R. P. White, *Prog. Inorg. Chem.*, 1988, **36**, 195.

17 A. Spencer and G. Wilkinson, *J. Chem. Soc., Dalton Trans.*, 1972, 1570.

18 M. Abe, Y. Sasaki, T. Yamaguchi and T. Ito, *Bull. Chem. Soc. Jpn.*, 1992, **65**, 1585; S. Ye, H. Akutagawa, K. Uosaki and Y. Sasaki, *Inorg. Chem.*, 1995, **34**, 4527.

19 J. A. Baumann, D. J. Salmon, S. T. Wilson, T. J. Meyer and W. E. Hatfield, *Inorg. Chem.*, 1978, **17**, 3342; J. A. Baumann, D. J. Salmon, S. T. Wilson and T. J. Meyer, *Inorg. Chem.*, 1979, **18**, 2472; J. A. Baumann, S. T. Wilson, D. J. Salmon, P. L. Hood and T. J. Meyer, *J. Am. Chem. Soc.*, 1979, **101**, 2916.

20 H. E. Toma, C. J. Cunha and C. Cipriano, *Inorg. Chim. Acta*, 1988, **154**, 63; H. E. Toma and C. J. Cunha, *Can. J. Chem.*, 1989, **67**, 1632; H. E. Toma and D. P. Alexiou, *Electrochim. Acta*, 1993, **38**, 975; H. E. Toma, F. M. Matsumoto and C. Cipriano, *J. Electroanal. Chem. Interfacial Electrochem.*, 1993, **346**, 261; S. Cosnier, A. Deronzier and A. Llobet, *J. Electroanal. Chem. Interfacial Electrochem.*, 1990, **280**, 213; D. Akashi, H. Kido, Y. Sasaki and T. Ito, *Chem. Lett.*, 1992, 143.

21 M. Abe, Y. Sasaki, Y. Yamada, K. Tsukahara, S. Yano and T. Ito, *Inorg. Chem.*, 1995, **34**, 4490; M. Abe, Y. Sasaki, Y. Yamada, K. Tsukahara, S. Yano, T. Yamaguchi, M. Tominaga, I. Taniguchi and T. Ito, *Inorg. Chem.*, 1996, **35**, 6724; H. E. Toma and K. Araki, *Coord. Chem. Rev.*, 2000, **196**, 307.

22 T. Ito, T. Hamaguchi, H. Nagino, T. Yamaguchi, J. Washington and C. P. Kubiak, *Science*, 1997, **277**, 660; K. Ota, H. Sasaki, T. Matsui, T. Hamaguchi, T. Yamaguchi, T. Ito, H. Kido and C. P. Kubiak, *Inorg. Chem.*, 1999, **38**, 4070; T. Ito, T. Hamaguchi, H. Nagino, T. Yamaguchi, H. Kido, I. S. Zavarine, T. Richmond, J. Washington and C. P. Kubiak, *J. Am. Chem. Soc.*, 1999, **121**, 4625; H. Kido, H. Nagino and T. Ito, *Chem. Lett.*, 1996, 745; T. Yamaguchi, N. Imai, T. Ito and C. P. K. Kubiak, *Bull. Chem. Soc. Jpn.*, 2000, **73**, 1205.

23 M. H. Wall, Jr., S. Akimoto, T. Yamazaki, N. Ohta, I. Yamazaki, T. Sakuma and H. Kido, *Bull. Chem. Soc. Jpn.*, 1999, **72**, 1475.

24 S. Davis and R. S. Drago, *Inorg. Chem.*, 1988, **27**, 4759; S. A. Fouda and G. L. Rempel, *Inorg. Chem.*, 1979, **18**, 1; S. A. Fouda, B. C. Y. Hui and G. L. Rempel, *Inorg. Chem.*, 1978, **17**, 3213.

25 (*a*) A. Ohto, A. Tokiwa-Yamamoto, M. Abe, T. Ito, Y. Sasaki, K. Umakoshi and R. D. Cannon, *Chem. Lett.*, 1995, 97; (*b*) K. Nakamoto, *Infrared and Raman Spectra of Inorganic and Coordination Compounds*, 4th edn., John Wiley & Sons, New York, 1986.

26 The expected molecular area of the trinuclear complex is calculated from crystal structure of a structurally similar, mixed-metal trinuclear complex $[Ru_2Mg(O)(CH_3CO_2)_6(cpy)_2(H_2O)]$, where cpy = 4-cyanopyridine: M. Abe, M. Tanaka and Y. Sasaki, manuscript in preparation.

27 A. J. Bard and L. R. Faulkner, *Electrochemical Methods*, *Fundamentals and Applications*, John Wiley & Sons, New York, 1980.
28 E. Laviron, *J. Electroanal. Chem. Interfacial Electrochem.*, 1974, **52**, 395.
29 M. Abe, Y. Sasaki, A. Nagasawa and T. Ito, *Bull. Chem. Soc. Jpn.*, 1992, **65**, 1411; M. Abe, M. Tanaka, K. Umakoshi and Y. Sasaki, *Inorg. Chem.*, 1999, **38**, 4146.
30 T. J. Lenk, V. M. Hallmark, C. L. Hoffmann and J. F. Rabolt, *Langmuir*, 1994, **10**, 4610; S.-W. Tam-Chang, H. A. Biebuyck, G. M. Whitesides, N. Jeon and R. G. Nuzzo, *Langmuir*, 1995, **11**, 4371; R. S. Clegg and J. E. Hutchison, *Langmuir*, 1996, **12**, 5239; H. Zhang, H. Xia, H. Li and Z. Liu, *Chem. Lett.*, 1997, 721; H.-Z. Yu, H.-L. Zhang, Z.-F. Liu, S. Ye and K. Uosaki, *Langmuir*, 1998, **14**, 619.
31 K. Uosaki, Y. Sato and H. Kita, *Langmuir*, 1991, **7**, 1510.
32 G. K. Rowe and S. E. Creager, *Langmuir*, 1991, **7**, 2307; H. C. De Long, J. J. Donohue and D. A. Buttry, *Langmuir*, 1991, **7**, 1991.
33 G. Inzelt and L. Szabo, *Electrochim. Acta*, 1986, **31**, 1381.
34 R. F. Crookson, *Chem. Rev.*, 1974, **74**, 5.
35 M. W. J. Beulen, F. C. J. M. van Veggel and D. N. Reinhoudt, *Chem. Commun.*, 1999, 503.
36 N. H. Koenig and D. Swern, *J. Am. Chem. Soc.*, 1957, **79**, 4235.
37 K. Uosaki, S. Ye and T. Kondo, *J. Phys. Chem.*, 1995, **99**, 14117.
38 T. Kondo, S. Horiuchi, I. Yagi, S. Ye and K. Uosaki, *J. Am. Chem. Soc.*, 1999, **121**, 391.
39 W. C. Wolsey, *J. Chem. Educ.*, 1973, **50**, A335.